Strain energy minimum and vibrational properties of single-walled aluminosilicate nanotubes

Suchitra Konduri, Sanjoy Mukherjee, and Sankar Nair*
School of Chemical & Biomolecular Engineering, Georgia Institute of Technology, Atlanta, Georgia 30332-0100, USA
(Received 10 April 2006; published 5 July 2006)

We study the origin of the strain energy minimum in a single-walled aluminosilicate nanotube via a harmonic force-constant model and molecular dynamics simulations. The model is based on a circular cross-section geometry of the nanotube composed of semirigid AlO_6 octahedra and SiO_4 tetrahedra. The monodispersity in the nanotube diameter is explained in terms of a minimum in the strain energy due to differences in bond energies on the inner and outer surfaces. The model also reproduces the diameter dependence of the radial breathing mode (RBM) frequency and is in accord with midinfrared spectroscopic characterization.

DOI: 10.1103/PhysRevB.74.033401 PACS number(s): 62.25.+g, 61.46.Fg, 63.22.+m

The synthesis, characterization, and applications of carbon-based and inorganic nanotube materials have been pursued extensively over the last decade.[1–3] Carbon nanotubes and their inorganic counterparts (e.g., BN, WS_2, MoS_2) are produced by electric arc discharge, laser ablation, or chemical vapor deposition processes.[1,3] On the other hand, the synthesis of inorganic oxide nanotubes is pursued mostly by a variety of low-temperature liquid phase chemical processes.[2] In general, control over nanotube diameter and monodispersity has remained a challenging task, partly because there has not appeared any obvious aspect of the formation mechanism[1,4,5] that allows facile control over nanotube curvature. Indeed, several theoretical and computational studies have shown that the strain energy of bending a graphitic sheet into a nanotube decreases monotonically with increasing nanotube diameter.[6,7] Thus, there is no inherent and tunable energy minimum that could be employed to produce nanotubes of desired diameter.

An exception to the above considerations is the unique single-walled aluminosilicate nanotube, imogolite.[8,9] The wall is a layer of aluminum hydroxide (gibbsite), with isolated silanol (≡Si-OH) groups bound to the inner surface. Imogolite nanotubes are synthesized from mildly acidic aqueous aluminosilicate precursor solutions between 25–100 °C. Based on several types of experimental evidence (nitrogen adsorption, x-ray diffraction, TEM, and dynamic light scattering),[10] it is accepted that synthetic imogolite nanotubes are highly monodisperse in diameter, irrespective of a substantially diverse range of synthesis conditions reported in the literature. The outer diameter of the nanotube is ~2.2 nm and its inner diameter is ~1 nm. The wall is composed of hexagonally arranged aluminum atoms connected by double oxygen bridges. On the outer surface, each oxygen is coordinated to two aluminum atoms and a hydrogen atom. On the inner surface the hydrogen atoms are replaced by silicon, with every three oxygens coordinated by one silicon. Figure 1(a) shows the hexagonal building unit with the pendant silanol group. The octahedrally coordinated aluminum atoms are well ordered and the axial unit cell dimension [Fig. 1(b)] of the nanotube is 0.85 nm. The number of aluminum atoms in the circumference (N) is necessarily an even number. No chiral properties have been observed, and the symmetry of the nanotube is that of the zigzag $(n,0)$ configuration of carbon nanotubes.[11] The chemical formula of the unit cell is $(Al_2SiO_7H_4)_N$.

In this Brief Report, we present the simplest quantitative model that can describe the physics governing control over the imogolite nanotube diameter. It was suggested early[9] that the curvature of the nanotube could be due to the differing energies of the Al-O and Si-O bonds. More recently, a minimum in the diameter-dependence of the energy of the imogolite nanotubes was observed in molecular dynamics (MD) simulations.[12] This minimum was observed at $N=32$, whereas synthesized imogolite samples have $N=24$. If the monodispersity of the nanotubes can be explained on the basis of a simplified strain energy model that takes into account the geometry of the Al-O and Si-O bonds, there exists the potential to produce guidelines for the synthesis of nanotube materials with tunable diameters based on the above criteria. Here we re-examine the energy minimum of the imogolite nanotube and the application of a simple strain energy model. We also show that such a model can be used to predict vibrational properties, in particular the radial breathing mode (RBM) frequency which is sensitive to the nanotube diameter and which has been studied extensively in carbon nanotubes.[13]

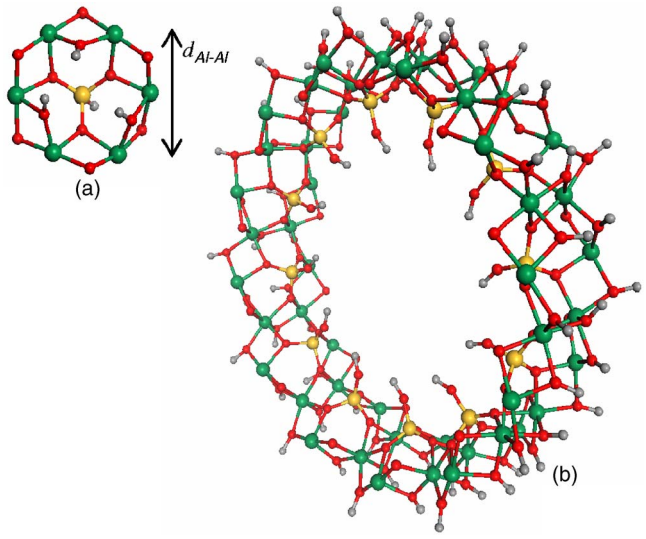

FIG. 1. (Color online) (a) Building unit of aluminosilicate nanotube showing hexagonal arrangement of aluminum atoms, bridging oxygens, and pendant silanol. (b) Perspective view of the unit cell of a nanotube with 24 aluminum atoms in the circumference. Green (dark gray); Al, Gold (light gray); Si, Red (black); O, Gray: H.

Aluminosilicate nanotube models with N ranging from 18 to 48 were built. The outer diameters of these nanotubes range between 1.5–4.5 nm. All simulations were performed on isolated nanotubes, since they are formed as isolated entities during the synthesis. With the c direction along the nanotube axis, the a and b dimensions of the unit cell are maintained at least 7 nm, to avoid any effects of intertube interactions. The individual nanotubes are also electrically neutral. The nanotube structures were first subjected to energy minimizations with a conjugate gradient algorithm, and the normal-mode vibrational frequencies were calculated. The RBM is clearly identified via the normal mode eigenvectors. The optimized structures were then subjected to NVT MD at 298 K with a 0.9 fs integration time step, a 5 ps equilibration stage, and a 100 ps data collection stage. The energy and temperature typically equilibrated within 1–2 ps. A Nosé-Hoover thermostat was used to control the temperature. The ensemble-average energy of the aluminosilicate nanotube was calculated as a function of its diameter from the MD trajectory, using five 20-ps blocks of data. The five values obtained were used to calculate an average energy and error bar, as shown in Fig. 2(a). We employed the recently developed CLAYFF force field,[14] since it has been shown to reproduce accurately the properties of a range of aluminosilicate minerals including gibbsite.[15] The force field is based on the Born ionic model, with fractional charges assigned to each atom and Lennard-Jones (12-6) potentials for Al-O, Si-O, and O-O interactions. The O-H bonds are described by a harmonic bond-stretching term. Nanotubes with $N \leqslant 16$ were unstable and disintegrated into amorphous structures. All MD calculations were carried out using the Discover (Accelrys Software, Inc.) module.

Figure 2(a) shows the total internal energy (potential and kinetic) per atom of the nanotube, as a function of the number of aluminum atoms (N) in the circumference of the nanotube. There is clearly a minimum in the internal energy per atom, a phenomenon that is not observed in carbon nanotubes or related inorganic nanotube materials. The depth of the energy minimum is substantial (about 0.4 kJ/mol/atom or 4.2 meV/atom) over the range of values of N studied here. On a per-atom basis, this well depth appears small compared to the thermal fluctuations ($kT \sim 25$ meV). However, such a comparison is misleading since the energy differences of complete nanotube units (for example, one unit cell which contains 336 atoms for $N=24$) are much larger than the thermal fluctuations. For instance, the low-temperature (α) form of quartz differs in internal energy from the high-temperature (β) form by only 0.63 meV/atom,[16] but a temperature of 850 K is required for the phase transition to occur. The energies are expressed here on a per-atom basis only to allow direct comparison of the strain energies of nanotubes of different diameters.

The inset of Fig. 2(a) shows the radius (R) of the nanotube as a function of N. For convenience, the radius is based on the average distance of the aluminum atoms from the nanotube axis, since they form the planar hexagonal sublattice of the nanotube wall. The radius follows a linear dependence on N. Figure 2(b) shows the RBM frequency (f_{RBM}) of the nanotube as a function of the radius. A power law dependence of the RBM is observed: $f_{\mathrm{RBM}}=40.93R^{-1.13}$. This approximate inverse dependence of the RBM frequency on the nanotube radius has also been predicted and observed in carbon nanotubes. It allows a characterization of nanotube diameters in carbon nanotube samples by Raman spectroscopy.[13] In the present system the synthesized nanotube samples are always monodisperse, obviating the need for RBM measurements. However, the RBM calculation offers an important test of the model presented below for explaining the radius dependence of the nanotube energy.

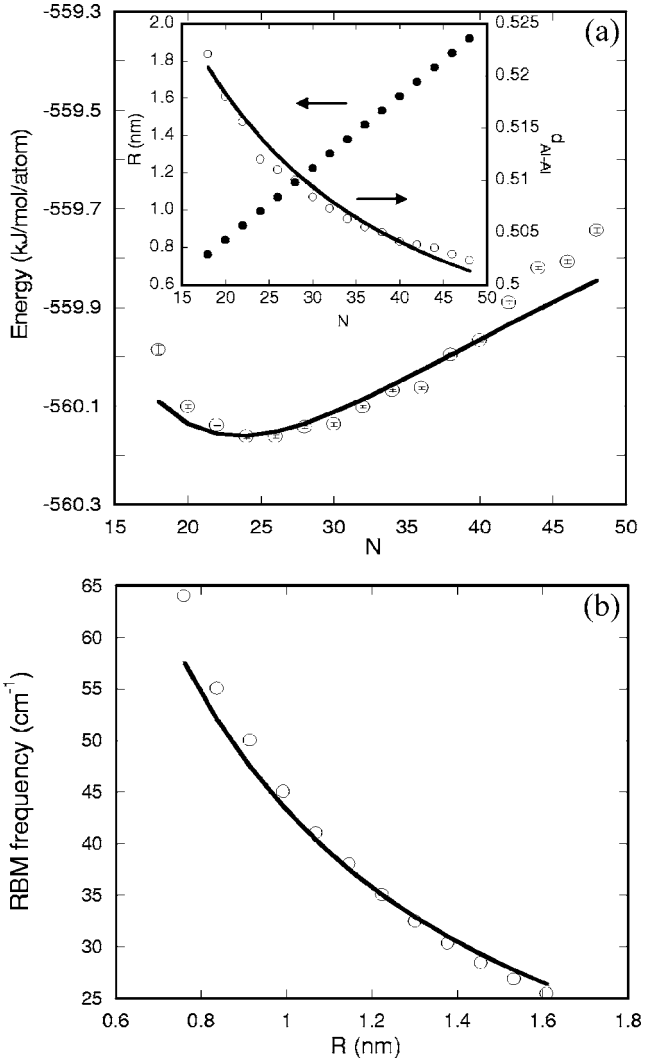

FIG. 2. (a) Total energy per atom at 298 K of the nanotube vs the number of aluminum atoms in the circumference. (Inset) Nanotube radius and distance $d_{\mathrm{Al\text{-}Al}}$ vs the number of aluminums in the circumference. (b) Radial breathing mode frequency vs nanotube radius. Symbols denote results of atomistic calculations and solid lines are model fits.

To model the strain energy of the nanotube, we assume that it has a circular cross section and is composed of "semi-rigid" aluminum octahedra and silicon tetrahedra, connected by oxygen atoms (Fig. 1). The octahedra and tetrahedra are assumed to maintain their ideal O-Al-O and O-Si-O bond angles (90° and 109.5°, respectively) but allow stretching of their Al-O and Si-O bonds. This model is thus in the spirit of

the "central force" models that have been developed for studying the properties of oxide materials.[17,18] In the simplest approximation, we model the bonds with harmonic bond stretching potentials

$$V_{\mathrm{Al-O}} = K_1(d_1 - d_{1e})^2 \quad \text{and} \quad V_{\mathrm{Si-O}} = K_2(d_2 - d_{2e})^2. \quad (1)$$

Here K_1 and K_2 are the force constants, d_1 and d_2 are the bond lengths in a nanotube of given radius, and d_{1e} and d_{2e} are the "equilibrium" bond lengths of the two types of bonds. The peripheral O-H bonds would make no contribution to the strain energy, and are not considered. For a nanotube with N aluminum atoms in the circumference, there are $4N$ Al-O bonds, $3N$ Si-O bonds and $14N$ atoms in the unit cell. Then the internal energy is given by a sum of strain-independent and strain-dependent terms

$$E(N) = E_0 + 4NK_1(d_1 - d_{1e})^2 + 3NK_2(d_2 - d_{2e})^2. \quad (2)$$

The strain-independent term contains the kinetic energy and the interatomic potential energies (e.g., O-H) that do not depend on the nanotube radius. This term is also directly proportional to the number of atoms in the nanotube. Hence, the energy per atom can be written as

$$\bar{E}(N) = E(N)/14N = \bar{E}_0 + (2/7)K_1(d_1 - d_{1e})^2 + (3/14)K_2(d_2 - d_{2e})^2. \quad (3)$$

Here, $\bar{E}_0$ is a constant. As the nanotube radius changes, the bond lengths obey well-defined geometric relationships dictated by the semirigidity of the tetrahedra and octahedra, and the assumption of a circular geometry. Using the geometry of Fig. 1, it can be easily shown that $d_1 = (2R/\sqrt{6})\sin(2\pi/N)$ and $d_2 = d_1/\sqrt{2}$. Also, N and R have the linear relationship obtained from the MD simulations, shown in the inset of Fig. 2(a). As a result, an important geometrical aspect of the model is the prediction that the distances between the aluminum atoms in the circumference decrease as N (and hence the radius R) increases. The inset of Fig. 2(a) compares the predicted distance $d_{\mathrm{Al\text{-}Al}}$ (see Fig. 1) to the simulation results, showing very good agreement.

Next, we derive an expression for the RBM frequency from $E(N)$. We consider a nanotube with a fixed N and instantaneous radius R, with all atoms undergoing a collective radial breathing vibration. In this case, the Lagrangian can be written as

$$L = \tfrac{1}{2}M\dot{R}^2 - 4NK_1(d_1 - d_{1e})^2 - 3NK_2(d_2 - d_{2e})^2. \quad (4)$$

Here the constant terms are not included, and the radius is employed as the generalized position coordinate. The unit cell mass is $M = N(2m_{\mathrm{Al}} + m_{\mathrm{Si}} + 7m_{\mathrm{O}} + 4m_{\mathrm{H}})$. The two bond lengths are functions of the instantaneous radius as given above. The harmonic RBM frequency is then calculated from the Lagrangian equation $d(\partial L/\partial \dot{R})/dt = \partial L/\partial R$, yielding the result,

$$\omega_{RBM} = 2\pi f_{RBM} = \sqrt{4N(4K_1 + 1.5K_2)/3M}\,\sin(2\pi/N). \quad (5)$$

The two expressions [Eqs. (3) and (5)] for $\bar{E}$ and f_{RBM} are then fitted simultaneously by nonlinear least squares to the data obtained from the MD simulations. The fitting parameters are d_{1e}, d_{2e}, K_1, K_2, and $\bar{E}_0$. The best fits for the equilibrium bond lengths are $d_{1e} = 0.200 \pm 0.005$ nm and $d_{2e} = 0.162 \pm 0.005$ nm. These are in accord with the nominal octahedral Al-O and tetrahedral Si-O bond lengths observed in oxide materials ($\sim$0.2 nm and $\sim$0.16 nm). The fitted values of the two harmonic constants are $K_1 = (2.43 \pm 0.02) \times 10^4$ kJ mol^{-1} nm^{-2} and $K_2 = (3.55 \pm 0.02) \times 10^4$ kJ mol^{-1} nm^{-2}. The RBM frequency is well reproduced as a function of the radius [Fig. 2(b)]. The theoretical prediction yields a power law fit $f_{\mathrm{RBM}} = 39.96R^{-0.97}$, which is in very good agreement with the power law obtained from the MD simulations. The fitted value of the strain-independent energy $\bar{E}_0$ is -562.274 ± 0.010 kJ mol^{-1}. Together, the parameters also yield a good fit of the strain energy in Fig. 2(a).

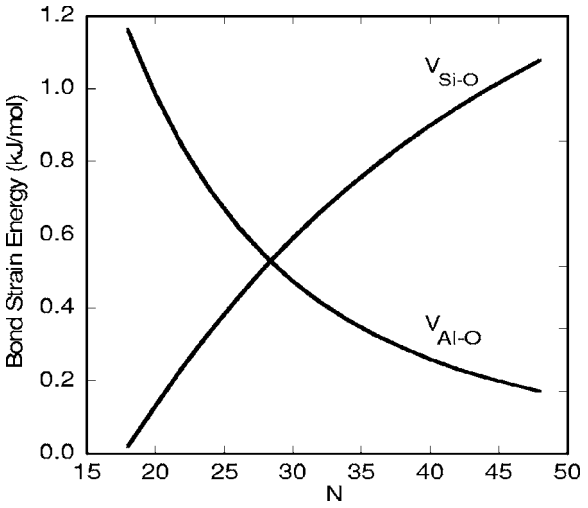

FIG. 3. Bond strain energies [Eq. (1)] of Al-O and Si-O vs the number of aluminum atoms in the circumference.

Figure 3 shows $V_{\mathrm{Al\text{-}O}}$ and $V_{\mathrm{Si\text{-}O}}$ [Eq. (1)] as a function of N, with the parameters obtained from the fits of Figs. 2(a) and 2(b). The contribution of $V_{\mathrm{Al\text{-}O}}$ to the total energy per atom $\bar{E}(N)$ [Eq. (3)] decreases monotonically with increasing nanotube radius, while that of the $V_{\mathrm{Si\text{-}O}}$ increases. If the inner and outer surfaces of the nanotube were identical, with no silanol groups bound on the inner surface, then the last term in Eq. (3) would not exist. $\bar{E}(N)$ would decrease monotonically with increasing N, and the lowest-energy structure is that of the planar gibbsite sheet. For the same reason, a graphene sheet has a lower energy than the carbon nanotube.[6,7] However, due to the functionalization of the inner surface with silanol groups, and the difference in Si-O and Al-O bond energies, a strain energy minimum is observed at $N = 24$, as shown in Fig. 2(a). This strain energy minimum, as well as the subsequent increase in strain energy as a function of nanotube radius, are predicted even by the simple harmonic force-constant model, and are unique features of the nanotube material under consideration here. According to the model prediction, the minimum at $N = 24$ corresponds to a nanotube diameter of 1.98 nm based on the aluminum atoms. Adding 2×0.14 nm $= 0.28$ nm for the oxygen atoms on the outer surface, the outer diameter of the

nanotube is predicted as 2.26 nm, which compares well with the experimental value of ~2.2 nm. The experimental value is based directly on TEM imaging and indirectly on center-to-center distances inferred from XRD patterns.[8–10] We also mention the difference between the energetics of the present system and that of framework materials like zeolites which are made up of corner-sharing SiO_4 tetrahedra. In the latter case, the flexibility (i.e., almost zero deformation energy) of the Si-O-Si linkages allows the formation of a large number of crystal structures of almost equal energy (e.g., Ref. 19). The synthesis can hence be easily directed to a particular structure by use of an organic structure-directing agent. In the nanotube, we encounter the opposite situation: the octahedra and tetrahedra are confined into a cylindrical geometry in which a change of diameter requires changes in bond lengths. This results in a substantial energy minimum and monodispersity of the diameter.

Additionally, we estimated the vibrational frequencies of the Al-O-Al and Al-O-Si linkages. Previous investigators have developed approximate analytical expressions for the stretching frequencies of atoms in solid-state networks, based on the central force model.[17,18] These predictions qualitatively agree with experimental infrared (IR) and Raman spectra. With the two force constants K_1 and K_2, it is possible to develop a similar analysis of the mixed-oxide nanotube composed of both AlO_6 octahedra and SiO_4 tetrahedra. We consider this detailed analysis to be outside the scope of the present Brief Report. However, we show here the physical significance of the force constants by calculating the frequencies of the "symmetric" stretching[18] vibrations of the oxygen atom in the Al-O-Al and Al-O-Si linkages. The calculated frequencies were found to be 583 cm^{-1} (Al-O-Al) and 1091 cm^{-1} (Al-O-Si), which are in the expected ranges for these linkages.[20]

Finally, we mention the analogous aluminogermanate nanotube,[20] synthesized by a simple substitution of Si with Ge in the reactant solution. It is also highly monodisperse with an outer diameter of ~3.3 nm (N=36).[10] MD simulations are currently not feasible due to the lack of reliable force-field parameters for Ge. The tetrahedral Ge-O bond has a weaker force constant than the Si-O bond. A weaker mismatch of Al-O and Ge-O bond energies is expected, and therefore a larger nanotube radius at the energy minimum, as can be predicted by Eq. (3). If the equilibrium bond lengths and force constants for different octahedral (tetrahedral) combinations of metal ions (layer and inner surface) can be estimated—from a force field, quantum chemical calculations, or experimental data—then the resulting nanotube dimensions can be predicted.

In summary, the unique energy minimum as well as several vibrational properties of the single-walled aluminosilicate nanotube (imogolite) can be explained via a simple harmonic force constant model of the strain energy. The force constant model allows at least a qualitative description of the essential physics governing the diameter control, and can be considered a good starting point for understanding the synthesis of the present class of single-walled metal oxide nanotube materials. Although more complicated models can be constructed (e.g., with O-Al-O and O-Si-O angle bending terms), the current results clearly show the potential for engineering the shape and dimensions of inorganic oxide nanomaterials by subtle control over interatomic bonding forces. Several such materials form in naturally occurring aqueous environments (e.g., hollow single-walled and double-walled aluminosilicate nanospheres[21]) and warrant close study of their structure and energetics.

We acknowledge support from the Petroleum Research Fund Grant No. 44074-G10 and the National Science Foundation CTS Grant No. 0403574.

*Corresponding author. Present address: School of Chemical & Biomolecular Engineering, Georgia Institute of Technology, 311 Ferst Drive NW, Atlanta, GA 30332-0100; FAX: 404-894-4200; electronic address: sankar.nair@chbe.gatech.edu

[1] M. S. Dresselhaus and H. Dai, MRS Bull. **29**, 237 (2004).
[2] M. Remskar, Adv. Mater. (Weinheim, Ger.) **16**, 1497 (2004).
[3] R. Tenne and C. N. R. Rao, Philos. Trans. R. Soc. London, Ser. A **362**, 2099 (2004).
[4] H. Ago, S. Ohshima, K. Tsukuagoshi, M. Tsuji, and M. Yumura, Curr. Appl. Phys. **5**, 128 (2005).
[5] C. Klinke, J. M. Bonard, and K. Kern, Phys. Rev. B **71**, 035403 (2005).
[6] D. H. Robertson, D. W. Brenner, and J. W. Mintmire, Phys. Rev. B **45**, 12592 (1992).
[7] H. Terrones and M. Terrones, New J. Phys. **5**, 126 (2003).
[8] L. A. Bursill, J. L. Peng, and L. N. Bourgeois, Philos. Mag. A **80**, 105 (2000).
[9] P. D. G. Cradwick, V. C. Farmer, J. D. Russell, C. R. Masson, K. Wada, and N. Yoshinaga, Nature (London), Phys. Sci. **240**, 187 (1972).
[10] S. Mukherjee, V. M. Bartlow, and S. Nair, Chem. Mater. **17**, 4900 (2005).
[11] R. Saito, G. Dresselhaus, and M. S. Dresselhaus, *Physical Properties of Carbon Nanotubes* (Imperial College Press, London, 1998).
[12] K. Tamura and K. Kawamura, J. Phys. Chem. B **106**, 271 (2002).
[13] M. S. Dresselhaus and P. C. Eklund, Adv. Phys. **49**, 705 (2000).
[14] R. T. Cygan, J. J. Liang, and A. G. Kalinichev, J. Phys. Chem. B **108**, 1255 (2004).
[15] See EPAPS Document No. E-PRBMDO-74-043627 for further details of the force field and the geometrical model. This document can be reached via a direct link in the online article's HTML reference section or via the EPAPS homepage (http://www.aip.org/pubservs/epaps.html).
[16] T. Demuth, Y. Jeanvoine, J. Hafner, and J. G. Angyan, J. Phys.: Condens. Matter **11**, 3833 (1999).
[17] M. F. Thorpe and F. L. Galeener, Phys. Rev. B **22**, 3078 (1980).
[18] F. L. Galeener, Phys. Rev. B **19**, 4292 (1979).
[19] K. D. Hammonds, H. Deng, V. Heine, and M. T. Dove, Phys. Rev. Lett. **78**, 3701 (1997).
[20] S. Wada and K. Wada, Clays Clay Miner. **30**, 123 (1982).
[21] L. A. Bursill, Mod. Phys. Lett. B **14**, 337 (2000).